ISSN 0001-4370, Oceanology, 2025, Vol. 65, No. 2, pp. 217–225. © Pleiades Publishing, Inc., 2025.

MARINE CHEMISTRY

Gas-Geochemical Features of Bottom Sediments in the Linear Depression Zone of the West Kara Stage

V. S. Sevastyanov[a, *], V. Yu. Fedulova[a], E. A. Moroz[b], E. A. Krasnova[a, c], S. G. Naimushin[a], N. V. Dushenko[a], S. A. Voropaev[a], and A. A. Dolgonosov[a]

[a] *Vernadsky Institute of Geochemistry and Analytical Chemistry, Russian Academy of Sciences, Moscow, Russia*

[b] *Geological Institute of Russian Academy of Sciences, Moscow, Russia*

[c] *Moscow State University, Moscow, Russia*

**e-mail: vsev@geokhi.ru*

Received April 8, 2024; revised May 28, 2024; accepted November 22, 2024

Abstract—During cruise 89 of the R/V *Akademik Mstislav Keldysh* in 2022, sediments cores were sampled at stations 7441 and 7444 in the southwestern Kara Sea. Station 7444 was located on a large submeridional depression, under the bottom of which gas-saturated sedimentary strata were detected. Background station 7441 was located 68 km from station 7444. For the sediments of the background station 7441, the ratio of hydrocarbon gases $C_1/C_{2+} < 100$ indicated their thermogenic nature. In the sediments at station 7441, the formation of the gas component in the sediments was due to degradation of OM and influx of thermogenic gases, while in the sediments of station 7444, there was an influx of biogenic gas, apparently from permafrost. The average CH_4 concentration in the sediments of station 7444 exceeded the average concentration in the sediments of core 7441 by 700 times, and the average CO_2 concentrations in the sediments of stations 7444 and 7441 were comparable. A sulfate–methane transition zone (SMTZ) was detected at the 541–545 cm horizon of the sediments of station 7444, where the sulfate concentration decreased to the minimum values, CH_4 and CO_2 concentrations reached maximum values. The sulfur isotopic composition of $\delta^{34}S$ in this region was +20.8‰. The biogenic nature of gas in the sediments of station 7444 was evidenced by low values of the carbon isotopic composition of CH_4 (mean value $\delta^{13}C(CH_4) = -99.7$‰) and high $C_1/C_{2+} > 10000$ ratio near the SMTZ.

Keywords: Kara Sea, sediments, organic matter, hydrocarbon gases, carbon isotope composition

DOI: 10.1134/S0001437024701078

INTRODUCTION

Arctic marine sediments contain large amounts of carbon, totaling 10^{15} g [19]. The continental shelf plays a significant role in the global carbon cycle, since the majority (80%) of organic carbon is buried on the shelf, which makes up 7.6% of the area of the World Ocean [11]. Diagenesis of organic matter (OM) leads to the emission of methane and CO_2 from marine sediments into the water column, then into the atmosphere, which can cause global warming. Moreover, the greenhouse effect of methane is 28 times stronger than that of CO_2 [17]. Rising temperatures cause permafrost to melt and gas hydrates to decompose. Temperature in the Arctic is rising four times faster than the global average [24]. It is suggested that gas hydrates will begin to actively decompose when the temperature of bottom water increases by 2°C [13]. The released gases migrate along faults to the seabed surface, leading to an increase in the concentration of hydrocarbon gases in sediments. Natural gas emission from the bottom on Arctic seas shelf and release of gas bubbles have been recorded in many Arctic regions [1, 2, 4, 9]. Seismoacoustic studies of the Kara Sea area revealed the presence of gas in the structure of the sedimentary cover and water column [7]. It appeared that "bright spot" type anomalies (an indicator of gas accumulation) on seismoacoustic records are often located above fault zones [4].

In [15, 16], it was shown that on the shelf of Korea in the Ulleung basin and on the Chukchi Sea shelf, marine sediments near the seep area contain a large amount of biogenic and thermogenic methane. There are a number of studies [12, 18, 21, 22] in which the distribution of gases in bottom sediments on the shelf in the area of seep fields was investigated. Studies of marine sediments near the Yamal Peninsula in the southern Kara Sea have shown that fluid migration and methane saturation of sediments occur as a result of the degradation of permafrost [23, 25].

The aim of the study was to identify gas-geochemical features in bottom sediments in the area of the submeridional depression in the southwestern Kara Sea. Since there are no data on the distribution of gases in the sedimentary cover of the rift structure of

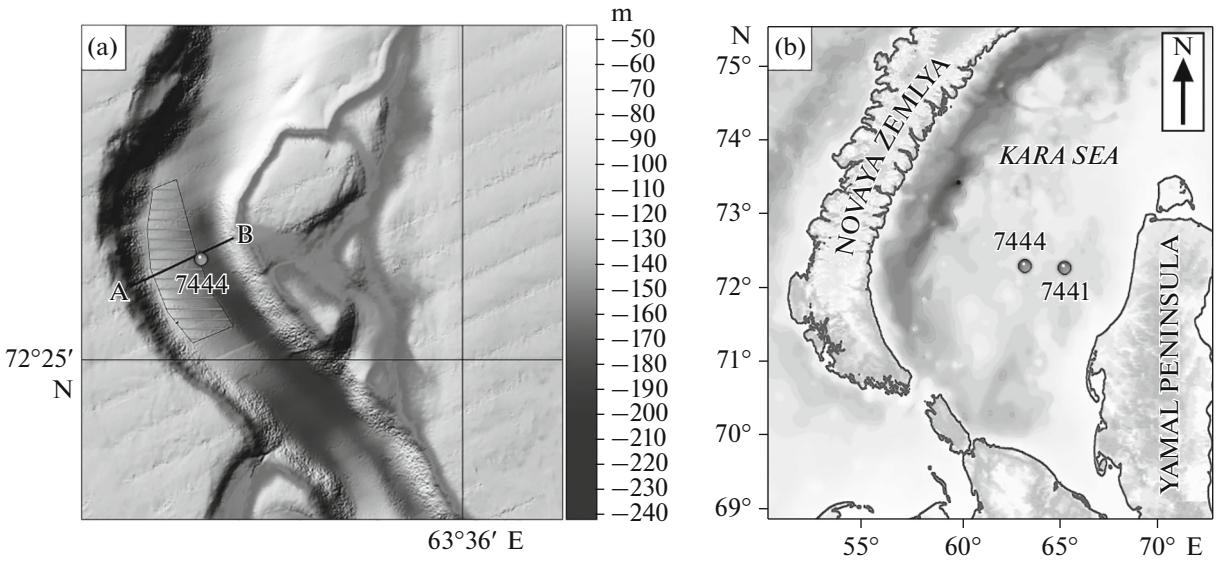

Fig. 1. Relief of test site (a) and map of location of sampling stations (b) in area of station 7444. Hatching shows projection of gas front onto bottom surface. A–B, line of acoustic profile (see Fig. 2).

the Novaya Zemlya Depression, the results will improve our understanding of the processes occurring during the gas migration through the sedimentary layer to the surface, better understand the carbon cycle in the Arctic seas, and anticipate future climate changes.

MATERIALS AND METHODS

Study Area and Geochemical Features of the Sedimentary Cover

During cruise 41 of the R/V *Akademik Nikolaj Strakhov* in 2019, studies were conducted at a test site in the southwestern Kara Sea and representing a large submeridional depression with a complexly constructed relief of the bottom and walls (Fig. 1a). The bottom surface was surveyed using a Reson Seabat 8111 multibeam echo sounder with a signal frequency of 100 kHz. Seismic profiling of the upper sedimentary section was carried out using an Edgetech 3300 nonparametric profiler with a modulated signal frequency of 2–12 kHz. According to high-frequency profiling data, signs of gas saturation of sedimentary strata were discovered in the bottom of the valley in the northern section: a so-called gas "pipe." During cruise 89 of the R/V *Akademik Mstislav Keldysh* in 2022 (Fig. 1b), a sediment core was collected in the central part of the sedimentary body at the bottom of the paleovalley at a sea depth of 225 m at station 7444. At a distance of 68 km from station 7444, background (comparison station) station 7441 (sea depth 110 m) was located on the West Kara step outside the zone of faults and linear depressions.

Analysis of the geomorphology of the study area allows us to establish the main stages of the development of the test sites relief in the Late Quaternary. By the beginning of the Quaternary, the study area was an erosion–denudation plain, significantly reworked during the Messinian regression [8]. During the Early Valdai glaciation, the test site was completely under ice cover, which blocked possible gas outlets to the surface along the existing zones of weakness at the bottom of the graben. During degradation of the glacier within the graben-shaped valley and in the southern part of the test site, subglacial channel flows functioned, producing significant erosive processing–erosion and transport of surface sediments, and rapid deepening of the valley. During the Middle Valdai (Karginian), the depression under study was flooded by the sea, and the retreat of the glacier, which was a natural barrier on the surface of the modern bottom, contributed to the activation of degassing processes. Furthermore, the final removal of the glacial load in the interval 13–11 thousand years ago apparently stimulated low-amplitude glacioisostatic movements along existing disjunctives.

RESEARCH METHODS

The sediments were collected using a multicorer (MC–Mini Muc K/MT 410, KUM, Germany) and a large-diameter gravity corer (LDG). The MC was used to recover sediments from the upper horizons up to 20–30 cm. Sediment cores from station 7444 (core length 626 cm) and station 7441 (core length 308 cm) were dark-gray silty-pelitic silts.

Gas Analysis

Wet marine sediments (300 mL) were placed in bottles (0.5 L) with a saturated NaCl solution, a 10 mL helium bubble was created in them, into which the

gases present in the sediments were extracted. The bottles were placed in an ultrasonic bath for 20 min, then in a drying oven heated to a temperature of 50–60°C for 12 h. The helium bubble with the extracted gases was transferred via syringe into a sealed 20 mL penicillin vial, previously filled with a saturated NaCl solution. The concentration of gases was measured using a CrystalLux-4000M gas chromatograph (Russia) with HP-Plot Q (30 m × 0.53 mm × 40 μm) and ZB-5 (30 m × 0.53 mm × 5 μm) capillary cores. The flow rate of the carrier gas, 6.0 grade helium, was 10 mL/min, and the thermostat temperature was 120°C. A flame ionization detector (FID) was used for analysis of hydrocarbon gases, and a flame photometric detector (FPD) was used for analysis of sulfur-containing gases. As a result, hydrocarbon gases (CH_4, C_2H_4, C_2H_6, C_3H_6, C_3H_8, C_4H_8, n-C_4H_{10}), CO_2, and CH_3SCH_3 were isolated.

The carbon isotopic composition ($\delta^{13}C$) of methane and carbon dioxide was measured at the Department of Geology and Geochemistry of Fossil Fuels of Moscow State University on a Delta V Advantage isotope ratio mass spectrometer (Finnigan, Germany), connected to a Trace GC Ultra gas chromatograph and an Isolink attachment with an oxidation reactor. A 0.1 mL gas sample was injected into the gas chromatograph. The gas components were separated in a CP-PoraPLOT capillary core (27.5 m × 0.32 mm × 10 μm) in a flow of the helium carrier gas at a temperature of 40°C. The sample then entered an oxidation reactor (a nickel tube filled with copper and nickel wire, periodically regenerated in an oxygen flow) heated to 1020°C, where the gas components were oxidized to carbon dioxide. The sample was fed through the ConFlo IV interface into the ion source of the mass spectrometer. The isotopic composition of carbon is expressed in ‰ relative to VPDB. The reproducibility of the analysis results, including the full cycle of sample preparation, does not exceed ±0.2‰ on average.

Organic Matter Analysis

OM isolated from the sediments into fractions was divided using a method developed at the laboratory of carbon geochemistry of the Vernadsky Institute of Geochemistry and Analytical Chemistry, Russian Academy of Sciences [6]. The sediments were dried at a temperature of 50° and ground in a ball mill (grinding fineness ≈60 μm), then OM was extracted from the sediments in a Soxhlet apparatus with a mixture of benzene and methanol (9 : 1 vol.) for 36 h. n-Pentane was added to the extracted OM sample in a 50-fold excess to separate asphaltenes. Then, the OM fractions were sequentially separated according to increasing polarity using liquid adsorption chromatography on ACSG with a fraction of 0.2–0.5 mm. A nonpolar hexane (H) fraction, three fractions of increasing polarity—hexane–benzene (HB), benzene (B), and benzene–methanol (BM) and asphaltenes (A) were isolated. The content of extracted OM in the sediments is given in units of mg g^{-1} dry sediments.

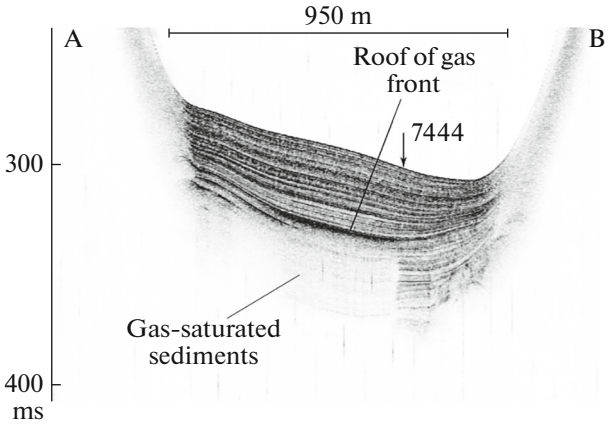

Fig. 2. High-frequency acoustic profile (2–12 kHz) along line A–B (see Fig. 1) with pronounced "bright spot" anomaly, recording hanging wall of gas front.

The isotopic composition of carbon in the extracted OM was measured using a Flash EA 1112 elemental analyzer (Thermo Scientific, Germany) coupled with a Delta Plus XP isotope ratio mass spectrometer (Thermo Fisher Scientific, Germany). The temperature of the oxidation reactor was 1020°C, and that of the reduction reactor, 650°C. The accuracy of the measurements was assessed using the international oil standard NBS 22 ($\delta^{13}C_{VPDB} = -29.7‰$). The standard deviation of the analysis was ±0.2‰. The obtained values of the carbon isotopic composition are presented as $\delta^{13}C$ with respect to the international standard VPDB.

RESULTS

On the seismoacoustic section in the area of station 7444, at a depth of about 18 m from the seabed surface, a clearly defined acoustic anomaly (like a "bright spot" or a so-called gas "pipe") was discovered, behind which the signal recording the roof of the gas front decayed (Fig. 2). The valley bottom is complicated by ramparts and trough. The largest feature on the valley bottom is a ridge extending more than 8 km along the depression—a shallow-water contourite drift. The width of the gas front along the section near station 7444 is about 580 m, which indicates the entry of gas into the sediments that make up most of the area of the bottom of the trough. The hanging wall area of the gas front is estimated at approximately 0.8 km^2. The areal gas anomaly identified by seismoacoustic data is related to the paleorelief and geological structure. In the Neogene–Quaternary, Paleozoic and Mesozoic rift structures of the Kara shelf experienced

Table 1. Vertical distribution of concentration and $\delta^{13}C$ for some gases of sediments of stations 7441 and 7444

Horizon, cm	Concentration, μg/L				$C_1/(C_2+C_3)$	$\delta^{13}C_{CH_4}$, ‰	$\delta^{13}C_{CO_2}$, ‰
	CH_4	C_2H_6	C_3H_8	CO_2			
Station 7441							
0–6	4.47	0.18	0.11	134	15.4	–*	–
6–10	3.04	0.39	0.35	190	4.12	–	–
10–14	2.23	0.43	0.13	158	3.96	–	–
14–18	1.21	4.82	0.36	113	0.23	–	–
10–14	1.36	0.28	0.71	97.7	1.38	–	–
34–38	1.00	0.37	0.28	121	1.54	–	–
57–61	1.03	0.29	0.40	155	1.50	–	–
105–109	1.79	0.40	0.41	506	2.21	–	–
121–125	1.25	0.25	0.16	340	3.01	–	–
171–175	1.88	0.35	0.37	1090	2.58	–	–
212–216	3.16	0.43	0.35	1610	4.05	–	–
260–264	3.67	0.44	0.35	1500	4.70	–	–
300–304	2.53	0.30	0.23	1690	4.76	–	–
Station 7444							
0–6	1.30	0.22	0.07	158	4.43	–	−18.5
6–10	1.43	0.16	0.13	33.1	4.92	–	−21.0
10–14	2.40	0.16	0.15	161	7.97	–	−14.7
14–18	4.36	0.19	0.14	199	12.9	–	−16.7
22–26	5.66	0.20	0.03	256	24.8	–	−15.8
14–18	2.46	0.20	0.18	200	6.43	–	−15.4
22–26	4.29	0.18	0.13	259	13.7	–	−15.7
52–56	18.7	0.28	0.25	608	35.4	–	−16.6
91–95	44.6	0.28	0.23	818	86.9	–	−15.9
125–129	68.6	0.26	0.19	228	151	−100.6	−16.6
175–179	88.3	0.32	0.27	651	150	−99.8	−16.2
195–199	118	0.30	0.18	1160	245	−100.9	−16.9
247–251	159	0.31	0.00	1450	507	−101.9	−19.3
285–289	209	0.31	0.00	1320	681	−97.4	−17.6
352–356	450	0.36	0.26	1610	736	−99.4	−17.7
419–423	1040	0.57	0.18	1820	1410	−99.7	−17.8
492–496	4820	0.85	0.25	2320	4390	−99.6	−18.7
541–545	10700	0.54	0.02	2970	19200	−97.4	−24.9
618–622	8440	0.53	0.19	3030	11700	−96.0	−17.3

*—measurements were not carried out for these horizons.

neotectonic movements [5] of negative sign, which led to the intensive subsidence of individual forms.

The vertical distribution of the concentration of some gases and isotopic composition of carbon CH_4 and CO_2 for sediments of stations 7441 and 7444 are given in Table 1.

Figure 3 shows that the CH_4 concentration increased with increasing sediment depth at station 7444 from 1.2 μg/L in the surface layers to a maximum of 1.1×10^4 μg/L at the 543 cm horizon. The CH_4 concentration with increasing sediment depth at background station 7441 increased by approximately four times (Fig. 3). At the same time, the average CH_4 concentration in the sediments of station 7444 exceeded the average concentration in the sediments of station 7441 by 700 times. In contrast, the average CO_2 concentrations

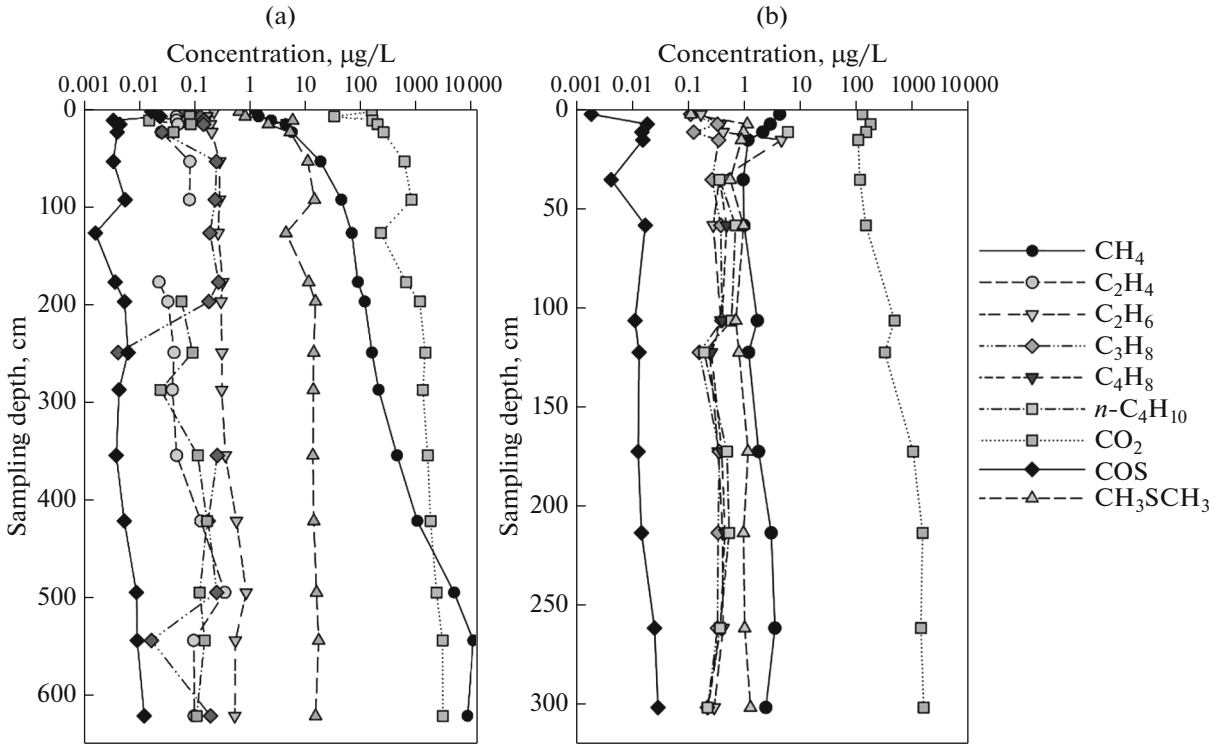

Fig. 3. Vertical distribution of gases in sediments of stations 7444 (a) and 7441 (b).

in the sediments of stations 7444 and 7441 were comparable. Determination coefficient R^2 between concentrations of CH_4 and CO_2 for sediments at stations 7441 and 7444 it was 0.36 and 0.84, respectively. Unsaturated hydrocarbon gases C_2H_4 and C_3H_6 in the sediments of station 7441 were absent, and the average concentration of CH_3SCH_3 by sediments core station 7441 was 10 times less than the concentration in the sediments of station 7444. In the sediments of station 7444 the isotopic composition of carbon is $\delta^{13}C(CH_4)$ varied from −96‰ at the 618–622 cm horizon to −101‰ at the 125–129 cm horizon, the value $\delta^{13}C(CO_2)$ at the 541–545 cm horizon was −24.9‰, while the average value for the core (19 horizons) was −17.5‰ (Table 1).

The vertical distribution of the amount of extracted OM in the sediments of stations 7441 and 7444 is shown in Fig. 4. The content of extracted OM in the sediments of station 7444 decreased by 5 times with an increase in the sediment depth and at the 40 cm horizon reached a constant level, coinciding with the amount of OM in the sediments of core station 7441.

Figure 5 shows change in the isotopic composition of carbon in extracted OM with sediment depth at stations 7441 and 7444. Clearly, $\delta^{13}C$ decreases in the sediment sequence (Fig. 5). At the same time, at a depth of 300 cm $\delta^{13}C$, the OM content in the sediments of station 7444 is ~1‰ higher than in sediments of station 7441.

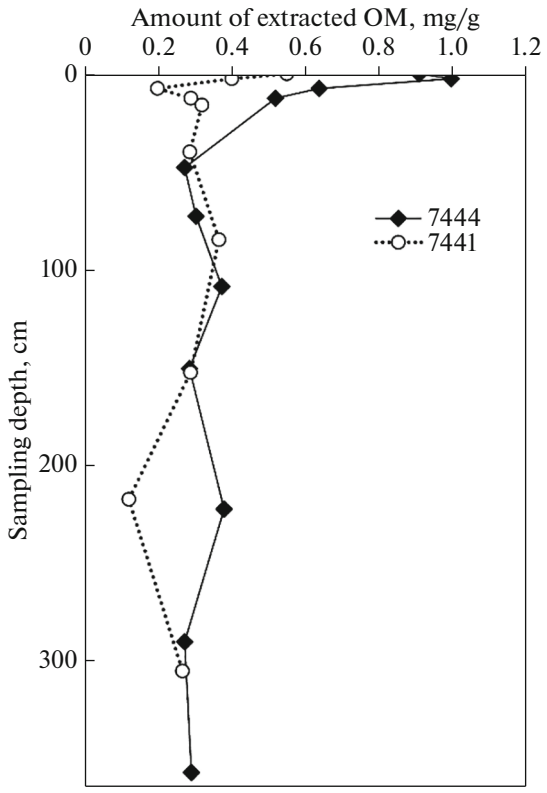

Fig. 4. Vertical distribution of extracted OM in sediments of stations 7441 and 7444.

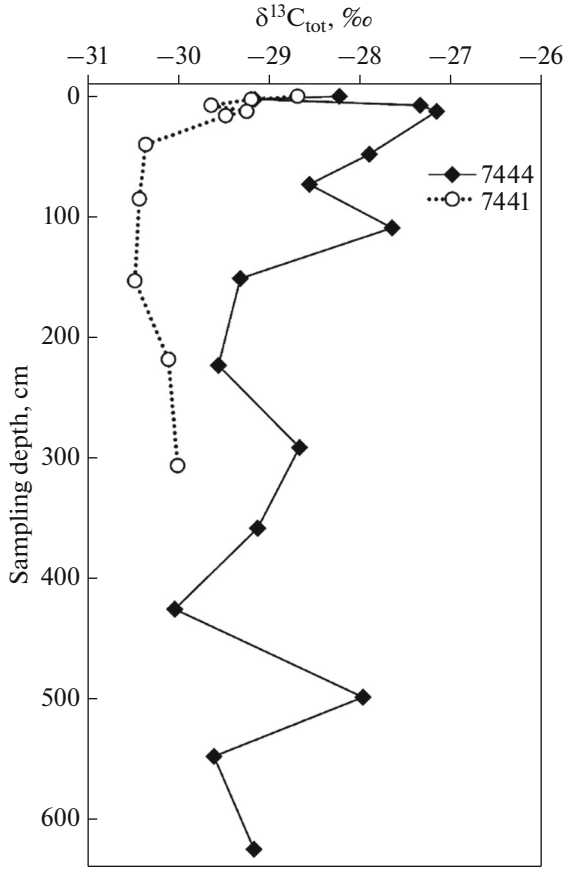

Fig. 5. Changes in isotopic composition of carbon in extracted OM with sediment depth at stations 7441 and 7444.

The vertical distribution of the content and $\delta^{13}C$ values of the OM fractions in sediments of stations 7441 and 7444 is presented in Table 2, which shows that the content of the A fraction decreases with increasing depth of sediment of station 7441 as a result of OM diagenesis. At the same time, the contents of the BM and B fractions remained virtually unchanged, while the contents of the H and HB fractions increased as a result of degradation of the A fraction. With an increase in sediment depth of core 7444, the contents of the A and BM fractions decreased slightly, while the contents of the H and HB fractions increased by approximately two times.

The main pattern of isotope fractional characteristics (IFC) of OM is a shift towards low $\delta^{13}C$ values with increasing sediment depth (Fig. 6).

DISCUSSION

According to the detailed multibeam bathymetric survey data, the depression in the area of station 7444 has the appearance of a graben-shaped valley with signs of significant fluvial reworking. According to high-frequency profiling data, the sedimentary cover at the bottom of the valley from top to bottom is composed of stratified, very acoustically permeable sediments that make up the drift body [3]. Seismoacoustic data recorded the rise of gas into thin-layered sediments at the turn of the Pleistocene and Holocene as a result of degradation of permafrost layers under postglacial transgression conditions. The vertical migration of hydrocarbon gases in the sediments is

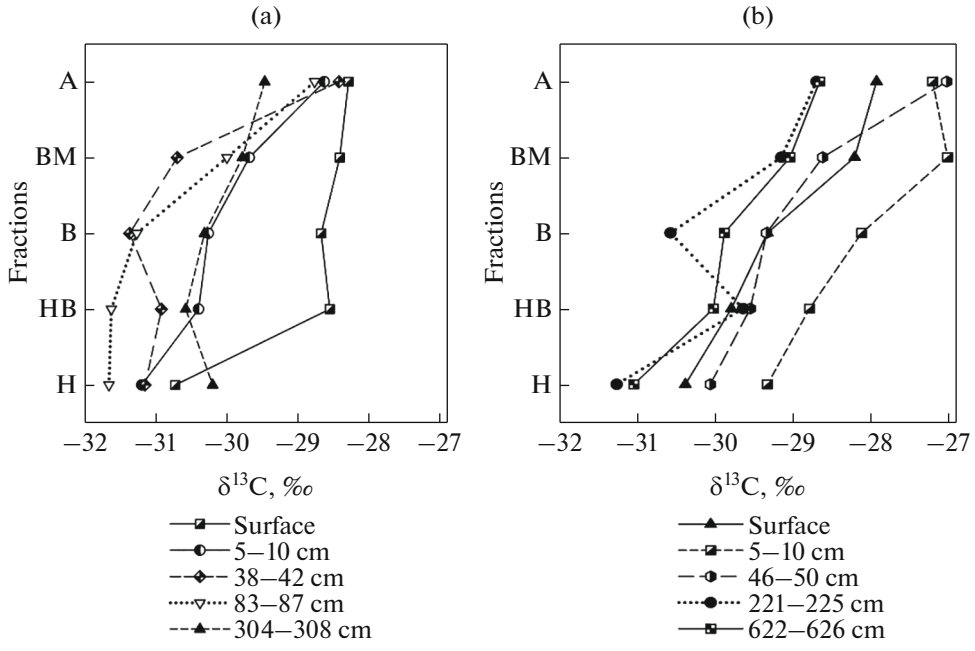

Fig. 6. Change in shape of isotope-fractional curves of some horizons with sediment depth at station 7441 (a) and 7444 (b).

Table 2. Vertical distribution of concentration and $\delta^{13}C$ from OM fractions in sediments of stations 7441 and 7444

Horizon, cm	$\delta^{13}C_{tot}$, ‰	Factions									
		H		HB		B		BM		A	
		$\delta^{13}C$, ‰	wt %	$\delta^{13}C$, ‰	wt %	$\delta^{13}C$, ‰	wt %	$\delta^{13}C$, ‰	wt %	$\delta^{13}C$, ‰	wt %
Station 7441											
Surface	−28.7	−30.7	7.8	−28.6	3.4	−28.7	8.3	−28.4	36.8	−28.3	43.7
0–5	−29.2	−31.2	7.1	−31.1	5.9	−30.3	6.8	−28.6	45.6	−28.5	34.6
5–10	−29.6	−31.2	7.5	−30.4	7.6	−30.3	8.6	−29.7	46.3	−28.6	30.0
10–15	−29.3	−30.7	14.6	−31.8	10.8	−31.1	8.1	−28.0	45.4	−28.2	21.1
14–18	−29.5	−31.3	9.2	−31.1	7.5	−28.7	11.7	−28.8	33.1	−29.1	38.5
38–42	−30.4	−31.1	20.6	−30.9	8.6	−31.4	7.8	−30.7	36.7	−28.4	26.3
83–87	−30.4	−31.7	25.2	−31.6	10.6	−31.3	6.6	−30.0	34.6	−28.8	23.0
151–155	−30.5	−31.6	19.2	−31.6	16.5	−31.5	7.2	−31.2	36.0	−27.0	21.1
216–220	−30.1	−30.7	23.9	−31.5	10.8	−31.7	9.2	−28.9	44.9	−30.1	11.2
304–308	−30.0	−30.2	21.3	−30.6	16.9	−30.3	7.2	−29.8	37.8	−29.5	16.8
Station 7444											
Surface	−28.2	−30.4	5.8	−29.8	3.8	−29.3	4.4	−28.2	38.6	−27.9	47.4
0–5	−29.2	−30.9	3.5	−30.7	2.2	−30.0	2.9	−29.0	49.8	−28.6	41.6
5–10	−27.3	−29.3	5.6	−28.8	5.2	−28.1	5.2	−27.0	39.6	−27.2	44.4
10–15	−27.2	−29.0	4.4	−29.7	3.9	−28.4	5.2	−26.8	44.1	−26.7	42.4
46–50	−27.9	−30.1	7.1	−29.6	1.0	−29.3	4.4	−28.6	43.1	−27.0	44.4
71–75	−28.6	−30.5	9.8	−30.1	8.2	−30.0	6.1	−27.7	38.2	−28.0	37.7
107–111	−27.7	−29.8	9.2	−29.5	7.1	−28.9	7.5	−27.4	33.8	−26.9	42.4
149–153	−29.3	−30.3	10.5	−30.1	13.0	−28.9	5.5	−28.9	39.0	−28.8	32.0
221–225	−29.6	−31.3	16.8	−29.6	18.1	−30.6	9.4	−29.2	30.2	−28.7	25.5
289–293	−28.7	−30.4	20.1	−30.4	6.6	−27.8	5.3	−27.9	36.4	−27.8	31.6
356–360	−29.1	−30.0	11.8	−29.6	9.0	−30.1	5.0	−29.0	33.5	−28.8	40.7
423–427	−30.0	−31.3	10.6	−31.8	11.8	−30.6	8.6	−29.4	30.8	−29.5	38.0
496–500	−28.0	−30.2	10.8	−29.9	10.2	−29.5	4.8	−28.0	35.5	−26.9	38.7
545–549	−29.6	−31.6	11.1	−30.3	6.4	−29.5	8.0	−29.6	28.7	−29.0	45.8
622–626	−29.2	−31.0	12.4	−30.0	6.2	−29.9	6.7	−29.0	34.9	−28.7	39.8

confirmed by their distribution over sediment depth (Fig. 3).

Hydrocarbon gases formed as a result of microbial reduction of CO_2, mainly composed of methane (C_1) and trace gases ethane (C_2) and propane (C_3) with the ratio $C_1/(C_2 + C_3) > 1000$ [16], since in this case significantly more methane is formed than ethane and propane. Conversely, thermogenic gases are mainly enriched in C_2 and C_3 and the ratio $C_1/(C_2 + C_3) < 100$ has been observed [26]. For sediment layers of station 7444 deeper than 125 cm, the ratio $C_1/(C_2 + C_3)$ reaches 10^2–10^4 (Table 1), which points to the biogenic nature of hydrocarbon gases in these sediments. However, in the surface horizons of station 7444, the ratio $C_1/(C_2 + C_3)$ becomes less than 100 as a result of microbial oxidation of CH_4. For sediments of station 7441 the ratio $C_1/(C_2 + C_3) < 100$ indicates the thermogenic nature of hydrocarbon gases. Also, from the classification by type of genesis [20], it follows that the hydrocarbon gases of sediments of station 7444 are microbiological nature. The average $\delta^{13}C(CH_4)$ value for station 7444 was –99.7‰. It should be noted that the of CH_3SCH_3 concentration is elevated in the sediments of station 7444, which is ten times higher than the concentration of CH_3SCH_3 in the sediments of station 7441 (Fig. 3). Typically, elevated dimethyl sulfide concentrations are associated with bacterial breakdown of compounds found in algae and cyanobacteria [14]. The accumulation of bacterial mass in the sediments of station 7444 is evidenced by the elevated concentration of extracted OM (Fig. 4) and increased values of $\delta^{13}C(OM)$ (Fig. 5). An uneven vertical change in $\delta^{13}C$ of the OM content

in the sediments of station 7444 is associated with a change in the molecular composition of OM over the sediment depth (Table 2). The high correlation coefficient $R^2 = 0.84$ between the CH_4 and CO_2 contents indicates migration of gases from a common source, a gas "pipe".

Basically, OM in marine sediments degrades due to reduction of sulfates: $2CH_2O + SO_4^{2-} \rightarrow 2HCO_3^- + H_2S$. In this case, methanogenesis occurs during the fermentation of acetate above the sulfate–methane transition zone (SMTZ) and reduction of CO_2 below the SMTZ. Anaerobic oxidation of methane $CH_4 + SO_4^{2-} \rightarrow HCO_3^- + HS^- + H_2O$ occurs near the SMTZ. Apparently, for the sediments of station 7441 down to the maximum sampling depth (308 cm), the SMTZ is not reached and the main OM decomposition reaction is that involving SO_4^{2-}. For sediments of station 7444 in the 541–622 cm layer, the CH_4 concentration reaches its maximum. In this layer, the $\delta^{13}C(CH_4)$ value has a maximum, and $\delta^{13}C(CO_2)$, a minimum (Table 1), as is usually the case in the area of the SMTZ. Similar patterns in the SMTZ were obtained for marine sediments of the Chukchi Sea and Sea of Japan [15, 16].

Usually, during diagenesis of OM in marine sediments, the A fraction formed by heterocyclic hydrocarbons degrades and the H and HB fractions form (increase in concentration) [10]. For sediments of station 7441, the correlation coefficient between the content of the H, HB fractions and the A fraction was $R^2 = 0.72$ and 0.61, respectively. The content of fraction A in the sediments of station 7444 (Table 2) remained virtually unchanged with the depth of the horizon, while the content of the H and HB fractions increased. This means that the gas composition in the sediments of station 7444 was mainly formed due to gas flow from a gas "pipe", not due to breakdown of the A fraction. It should be noted that the OM contents in the sediments of stations 7441 and 7444 below the 40 cm horizon are practically the same (Fig. 4), while the CH_4 content remained constant throughout the entire depth of the sediments of station 7441.

It is known that for the IFC of OM in marine sediments, the dependence $\delta^{13}C(A) > \delta^{13}C(BM) > \delta^{13}C(B) > \delta^{13}C(HB) > \delta^{13}C(H)$ exists, which was described by Academician E.M. Galimov [10]. It was found that for a fixed horizon of the sediment of stations 7441 and 7444, the following rule is observed: $[\delta^{13}C(A) > \delta^{13}C(BM) > \delta^{13}C(B) > \delta^{13}C(HB) > \delta^{13}C(H)]_{7444} > [\delta^{13}C(A) > \delta^{13}C(BM) > \delta^{13}C(B) > \delta^{13}C(HB) > \delta^{13}C(H)]_{7441}$. This means that OM in the sediments of station 7441 is more transformed. The characteristic appearance of the IFC of OM at both stations is associated with the specific features of the diagenetic transformation of OM in sediments.

CONCLUSIONS

The data obtained indicate that station 7444 is located on the floor of a valley, which is a large submeridional depression in the southwestern Kara Sea. The formation of a layered sedimentary strata can be attributed to exogenic paleogeographic processes. Sedimentary strata are saturated with hydrocarbon gases and CO_2, presumably associated with permafrost degradation. Migration of gases leads to their accumulation in the fault zone and the formation of vertical gas "pipes". Low $\delta^{13}C$ values indicated the biogenic origin of hydrocarbon gases in the sediments of station 7444, $C(CH_4)$ from −101 to −96‰, and a high ratio of hydrocarbon gases $C_1/(C_2 + C_3) > 10000$ in the 541–622 cm sediment layer of station 7444. In this region, the CH_4 concentration reached a maximum of 1.1×10^4 μg/L. For the sediments of background station 7441, a ratio $C_1/(C_2 + C_3) < 100$ was obtained, indicating the thermogenic nature of hydrocarbon gases. The main behaviorial patterns of hydrocarbon gases in sediments are associated with the sources of gas input to sediments at stations 7444 and 7441.

ACKNOWLEDGMENTS

The authors thank leader of the expedition M.D. Kravchishina and the crew of the R/V *Akademik Mstislav Keldysh* for their assistance in conducting the research.

FUNDING

The study was supported by a grant from the Russian Science Foundation (project no. 23-27-00296).

ETHICS APPROVAL AND CONSENT TO PARTICIPATE

This work does not contain any studies involving human and animal subjects.

CONFLICT OF INTEREST

The authors of this work declare that they have no conflicts of interest.

REFERENCES

1. R. A. Ananiev, N. N. Dmitrevsky, A. G. Roslyakov, et al., "Acoustic monitoring of gas emission processes in the Arctic shelf seas," Oceanology **62** (1), 127–132 (2022).
2. B. V. Baranov, L. I. Lobkovsky, K. A. Dozorova, et al., "The fault system controlling methane seeps on the shelf of the Laptev Sea," Dokl. Earth Sci. **486**, 571–574 (2019).
3. B. V. Baranov, A. K. Ambrosimov, E. A. Moroz, et al., "Late quaternary contourite drifts on the Kara Sea shelf," Dokl. Earth Sci. **511**, 710–715 (2023).

4. V. G. Bondur and T. V. Kuznetsova, "Detecting gas seeps in Arctic water areas using remote sensing data," Izv. Atmos. Ocean. Phys. **51**, 1060–1072 (2015).
5. M. L. Verba, "Modern bilateral extension of the Earth's crust in the Barents-Kara region and its role in assessing oil and gas potential," Neft. Geol. Teor. Prakt. **2**, 1–37 (2007).
6. E. M. Galimov and L. A. Kodina, *Study of Organic Matter and Gases in Bottom Sediments of the World Ocean* (Nauka, Moscow, 1982).
7. A. P. Denisova, E. A. Moroz, E. A. Sukhikh, et al., "Signs of deep degassing in the upper part of the sedimentary cover of the shelf and water column of the Kara Sea," in *Geology of Seas and Oceans: Proc. XXIV Int. Sci. Conf. (School) on Marine Geology* (Inst. Okeanol. Ross. Akad. Nauk, Moscow, 2021), Vol. IV, pp. 235–239.
8. E. E. Musatov, "Paleovalleys of the Barents-Kara shelf," Geomorfologiya, No. 2, 90–95 (1998).
9. S. Yu. Sokolov, E. A. Moroz, G. D. Agranov, et al., "Manifestations of degassing in the upper part of the Pechora Sea sediment section and its relation to tectonics," Dokl. Earth Sci. **499**, 605–610 (2021).
10. E. M. Galimov, "Isotope organic geochemistry," Org. Geochem. **37** (10), 1200–1262 (2006). https://doi.org/10.1016/j.orggeochem.2006.04.009
11. J. I. Hedges and R. G. Keil, "Sedimentary organic matter preservation: An assessment and speculative synthesis," Mar. Chem. **49**, 81–115 (1995). https://doi.org/10.1016/0304-4203(95)00008-f
12. K. M. Hilligsoe, J. B. Jensen, T. G. Ferdelman, et al., "Methane fluxes in marine sediments quantified through core analyses and seismo-acoustic mapping (Bornholm Basin, Baltic Sea)," Geochim. Cosmochim. Acta **239**, 255–274 (2018). https://doi.org/10.1016/j.gca.2018.07.040
13. W. L. Hong, M. E. Torres, J. Carroll, et al., "Seepage from an Arctic shallow marine gas hydrate reservoir is insensitive to momentary ocean warming," Nat. Commun. **8**, 15745 (2017). https://doi.org/10.1038/ncomms15745
14. M. D. Keller, W. K. Bellows, and R. R. Guillard, "Dimethyl sulfide production in marine phytoplankton," in *Biogenic Sulfur in the Environment*, Ed. by E. S. Saltzman and W. J. Cooper (Am. Chem. Soc., Washington, D.C., 1989), pp. 167–182.
15. J. H. Kim, M. E. Torres, J. Choi, et al., "Inferences on gas transport based on molecular and isotopic signatures of gases at acoustic chimneys and background sites in the Ulleung Basin," Org. Geochem. **43**, 26–38 (2012). https://doi.org/10.1016/j.orggeochem.2011.11.004
16. J. H. Kim, A. Hachikubo, M. Kida, et al., "Upwarding gas source and postgenetic processes in the shallow sediments from the ARAON Mounds, Chukchi Sea," J. Nat. Gas Sci. Eng. **76**, 103223 (2020). https://doi.org/10.1016/j.jngse.2020.103223
17. S. Mau, M. Romer, M. E. Torres, et al., "Widespread methane seepage along the continental margin off Svalbard—from Bjørnøya to Kongsfjorden," Sci. Rep. **7**, 42997 (2017). https://doi.org/10.1038/srep42997
18. A. Mazumdar, H. M. João, A. Peketi, et al., "Geochemical and geological constraints on the composition of marine sediment pore fluid: Possible link to gas hydrate deposits," Mar. Pet. Geol. **38**, 35–52 (2012). https://doi.org/10.1016/j.marpetgeo.2012.07.004
19. A. D. McGuire, L. G. Anderson, T. R. Christensen, et al., "Sensitivity of the carbon cycle in the Arctic to climate change," Ecol. Monogr. **79**, 523–555 (2009). https://doi.org/10.1890/08-2025.1
20. A. V. Milkov and G. Etiope, "Revised genetic diagrams for natural gases based on a global dataset of >20,000 samples," Org. Geochem. **125**, 109–120 (2018). https://doi.org/10.1016/j.orggeochem.2018.09.002
21. H. Niemann, M. Elvert, M. Hovland, et al., "Methane emission and consumption at a North Sea gas seep (Tommeliten area)," Biogeosciences **2**, 335–351 (2005). https://doi.org/10.5194/bg-2-335-2005
22. J. W. Pohlman, M. Riedel, J. E. Bauer, et al., "Anaerobic methane oxidation in low-organic content methane seep sediments," Geochim. Cosmochim. Acta **108**, 184–201 (2013). https://doi.org/10.1016/j.gca.2013.01.022
23. A. Portnov, A. J. Smith, J. Mienert, et al., "Offshore permafrost decay and massive seabed methane escape in water depths >20 m at the South Kara Sea shelf," Geophys. Res. Lett. **40**, 3962–3967 (2013). https://doi.org/10.1002/grl.50735
24. M. Rantanen, A. Y. Karpechko, A. Lipponen, et al., "The Arctic has warmed nearly four times faster than the globe since 1979," Commun. Earth Environ. **3**, 168 (2022). https://doi.org/10.1038/s43247-022-00498-3
25. P. Semenov, A. Portnov, A. Krylov, et al., "Geochemical evidence for seabed fluid flow linked to the subsea permafrost outer border in the South Kara Sea," Geochemistry **80**, 125509 (2020). https://doi.org/10.1016/j.chemer.2019.04.005
26. M. J. Whiticar, "Carbon and hydrogen isotope systematics of bacterial formation and oxidation of methane," Chem. Geol. **161**, 291–314 (1999). https://doi.org/10.1016/S0009-2541(99)00092-3